Modelling Dendritic Solidification with Back Diffusion

The solidification of multicomponent alloys is a complex process controlled by the interplay of thermodynamic driving forces and solute transfer kinetics. Traditional models[1] are based on the assumption that solute diffusion is infinitely fast in the liquid, and consider two limiting cases for the diffusion in the solid, or back diffusion. If the back diffusion is also assumed to be infinitely fast, an equilibrium model, often referred to as the lever rule approach,[1] is obtained. Neglecting the back diffusion leads to the nonequilibrium Scheil-Gulliver model,[1] which is a more appropriate description in many cases.[2,3] However, in some alloys, for example single crystal Ni-based superalloys and steels, the Scheil-Gulliver approximation clearly breaks down and, to model solidification accurately, back diffusion must be accounted for. Furthermore, adding back diffusion to such cases is essential to predict the changes in microsegregation and the nature and amount of secondary phases formed as a function of the cooling conditions,[4] which in turn is critical to determine the properties of the alloy.[5,6] This report provides an overview of the model used in JMatPro to calculate the effect of back diffusion on the dendritic solidification of multicomponent alloys.

Model Description

The model is based on the following assumptions:

- The shape of the dendrite is approximated by one of three possible geometries: plate, cylinder, or sphere, respectively characterised by the coefficient $g = 0,1,2$. The concentration profiles are assumed to vary only along the length of the plate, or the radius of the cylinder or sphere, so that, in all cases, the microsegregation domain can effectively be treated as one-dimensional. The domain length is taken as half of the secondary dendrite arm spacing, λ, and the position along the relevant direction is denoted r.
- Only one solid phase is included in the calculation of back diffusion. Formation of secondary phases is dealt with separately and leads to two steps in the model. The first step involves the thermodynamic calculation of all the phases that grow from the liquid at temperature T. The secondary phases obtained are then rejected from the system and an isothermal diffusion step follows, in which only the primary solid phase and the remaining liquid are considered. The duration of this step, Δt, is determined from the cooling rate, $\dot{T}$, and temperature step, ΔT, input by the user.
- Local equilibrium is assumed at the solid/liquid interface, i.e., the interfacial concentrations in the solid (S) and liquid (L) phases, respectively denoted C_{Si}^* and C_{Li}^* for component i ($i = 1, \dots, N$), are related via thermodynamic equilibrium conditions.[1,4]
- Solute diffusion in the liquid is taken as infinitely fast and, thus, the concentration in the liquid phase is uniform, i.e., $C_{Li}(r) = C_{Li}^*$. In the solid, on the other hand, solute diffusion is considered finite and governed by Fick's second law.[7,8] Inter-solute terms are neglected and an Arrhenius form is assumed for the diffusion coefficients:[7]

$$D_i = D_i^0 \exp\left(-\frac{Q_i}{RT}\right) \tag{1}$$

  In the above expression, D_i^0 denotes a frequency factor, Q_i a molar activation energy, and $R = 8.3144\ \text{J mol}^{-1}\ \text{K}^{-1}$ is the gas constant.
- During the isothermal diffusion step there is no solute flow into or out of the dendritic domain. The sum of the molar fractions of the solid and liquid phases, $f_T = f_S + f_L$, and the average concentration of each component in the dendrite, C_{Ti}, are determined beforehand in the thermodynamic calculation step and can only change in the next step, upon decreasing the temperature.

- The difference between the molar volumes of the solid and liquid phases is considered to be small enough so that a simple relationship between the position of the solid/liquid interface, r^*, and the molar fraction of solid, f_S, can be used:

$$f_S = f_T \left(\frac{r^*}{\lambda}\right)^{g+1} \tag{2}$$

- Dendrite tip undercooling and coarsening effects are neglected.

The above considerations essentially prescribe treating the growth of the primary solid phase as a diffusion with a moving boundary problem, while for the secondary phases the Scheil-Gulliver model is used. The evolution of the concentration profile for component i in the primary solid, $C_{Si}(r)$, is governed by the equation:[8]

$$\frac{\partial C_{Si}}{\partial t} = D_i \left(\frac{\partial^2 C_{Si}}{\partial r^2} + \frac{g}{r}\frac{\partial C_{Si}}{\partial r}\right), \; 0 \le r \le r^* \tag{3}$$

At the centre of the dendrite ($r = 0$), a zero-flux boundary condition is used,

$$\frac{\partial C_{Si}}{\partial r} = 0 \tag{4}$$

while at the solid/liquid interface ($r = r^*$), local equilibrium conditions are imposed:[1,4]

$$C_{Si}^* = k_i C_{Li}^* \tag{5}$$

The interfacial concentrations in the solid and liquid phases are, thus, related via equilibrium partition coefficients, k_i, which are fixed for the duration of the isothermal diffusion step, but are allowed to vary between steps.

The diffusion equations are coupled by requiring conservation of solute,

$$f_S\langle C_{Si}\rangle + f_L C_{Li}^* = f_T C_{Ti} \tag{6}$$

and ensuring that the liquid composition rests on the liquidus isotherm at temperature T:

$$T = T_m + \sum_{i=2}^{N} m_i C_{Li}^* \tag{7}$$

This guarantees that the position of the interface is the same for every component in the alloy. In the above expressions, T_m denotes the melting point of the pure solvent (labelled by $i = 1$), $m_i = \partial T/\partial C_{Li}^*$ the liquidus slopes,[1] and the average concentrations in the solid are calculated as

$$\langle C_{Si}\rangle = \frac{g+1}{(r^*)^{g+1}} \int_0^{r^*} C_{Si}(r) r^g \, dr \tag{8}$$

Solution of the coupled set of nonlinear equations (3), (6), and (7) provides the interface growth over the time step Δt, the updated solute concentration profiles in the solid, as well as the composition of the remaining liquid, which is used as the basis for the next isothermal step.

Case Studies

Figure 1 shows a comparison of the fraction solid vs temperature curves obtained using equilibrium, Scheil-Gulliver, and back diffusion models for different types of alloys often considered in casting simulations: AA356 (Al-0.01Cu-0.2Fe-0.3Mg-0.02Mn-7Si-0.1Zn wt%), AA7075 (Al-0.23Cr-1.6Cu-0.5Fe-2.5Mg-0.3Mn-0.4Si-5.6Zn wt%), ZMC711 (Mg-1.25Cu-0.75Mn-6.5Zn wt%), and NiFe 718 (Ni-0.5Al-19Cr-18.5Fe-3Mo-5.1Nb-0.9Ti-0.04C wt%). The back diffusion calculations were performed assuming a cylindrical dendrite geometry and using a cooling rate of 0.1 °C/s. For the investigated Al alloys, AA356 and AA7075, this leads to a secondary dendrite arm spacing of about 150 μm.[9] The same value was assumed for the Mg alloy ZMC711, but for Ni and Ni-Fe-based superalloys a secondary dendrite arm spacing of 100 μm is more common at the same cooling rate,[10] and this lower value was chosen in the case of alloy NiFe 718. As can be seen in the figure, for all these alloys the back diffusion result follows closely the Scheil-Gulliver one. This can be qualitatively understood by the low liquidus temperature and/or wide freezing range, which quickly reduce possible back diffusion as diffusion coefficients decrease exponentially with temperature.

For certain material types and alloy compositions, the above argument does not hold and back diffusion plays a significant role during solidification. Figure 2 illustrates this effect by comparing the fraction solid vs temperature curves obtained using equilibrium, Scheil-Gulliver, and back diffusion models for the Ni-based superalloys Udimet 720Li (Ni-2.5Al-14.7Co-16Cr-3Mo-5Ti-1.25W-0.015B-0.01C wt%) and René N6 (Ni-5.75Al-12.5Co-4.2Cr-0.15Hf-1.4Mo-5.4Re-7.2Ta-6W wt%). In the back diffusion calculations, a cylindrical shape was taken for the dendrite geometry, the cooling rate was set to 0.1 °C/s, and a

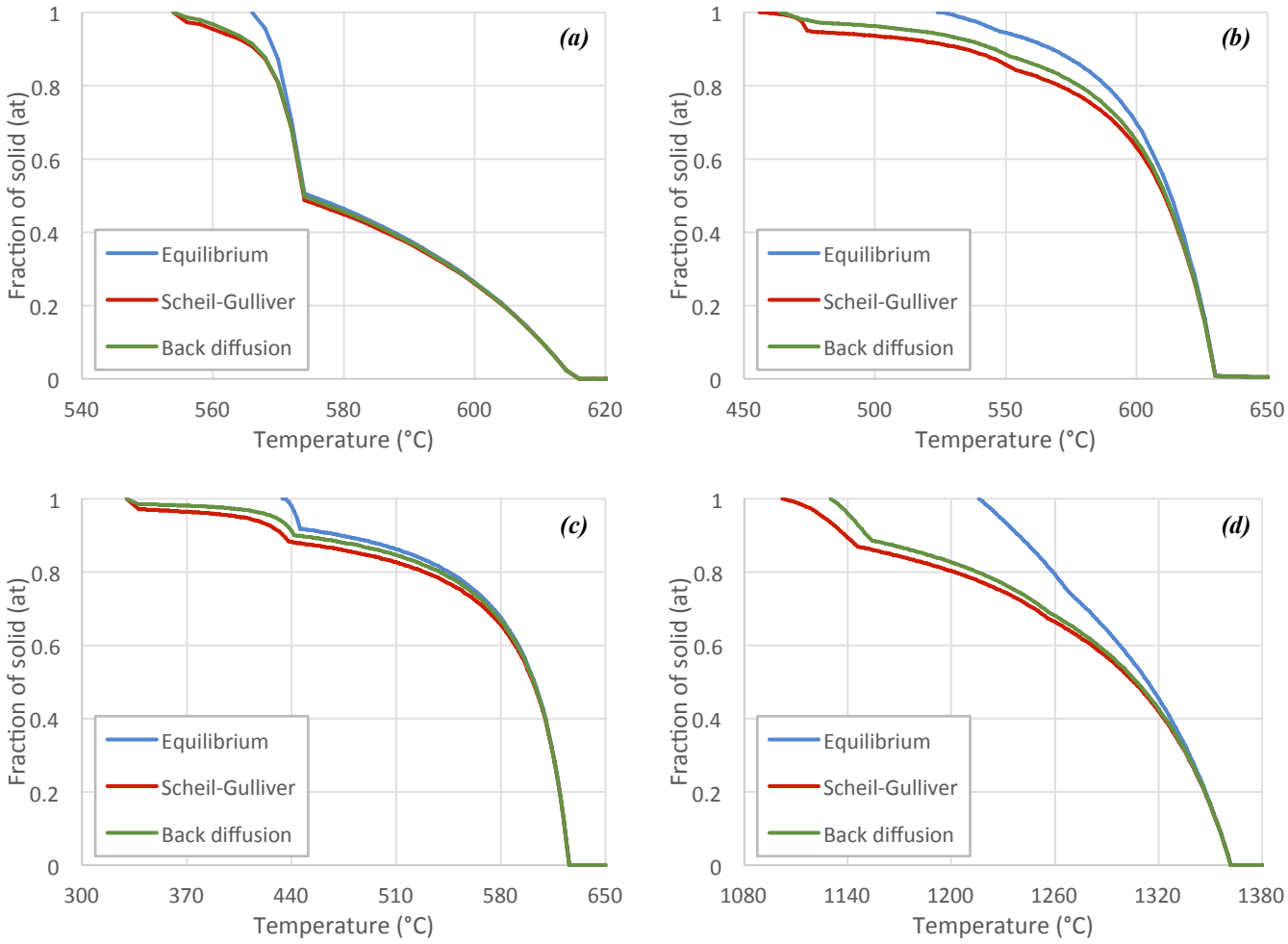

Figure 1: *Total fractions of solid calculated as a function of temperature using equilibrium, Scheil-Gulliver, and back diffusion models for different alloys: (a) AA356, (b) AA7075, (c) ZMC711, and (d) NiFe 718.*

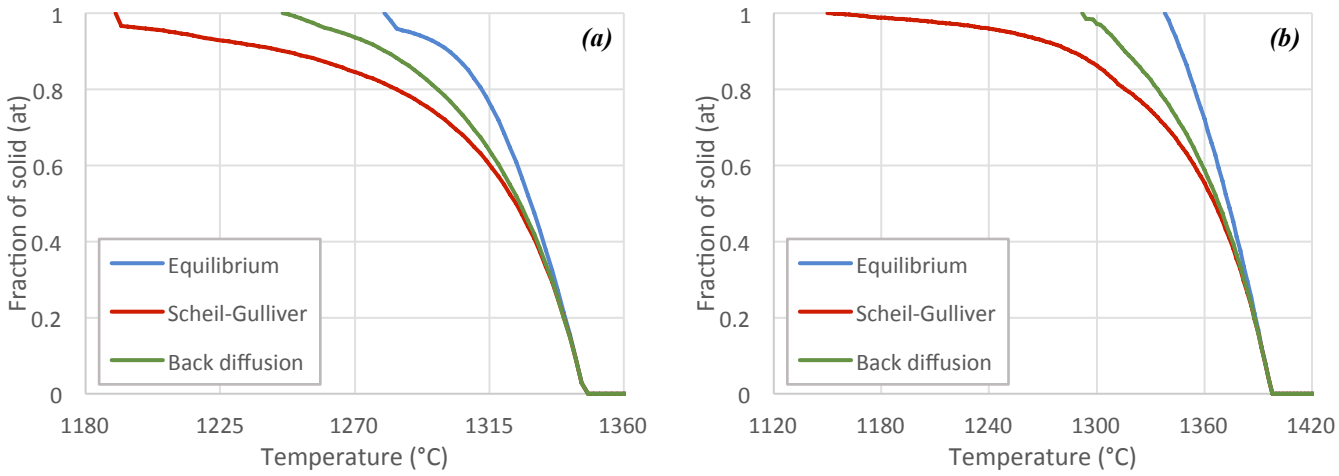

Figure 2: *Total fractions of solid calculated as a function of temperature using equilibrium, Scheil-Gulliver, and back diffusion models for the Ni-based superalloys Udimet 720Li (a) and René N6 (b).*

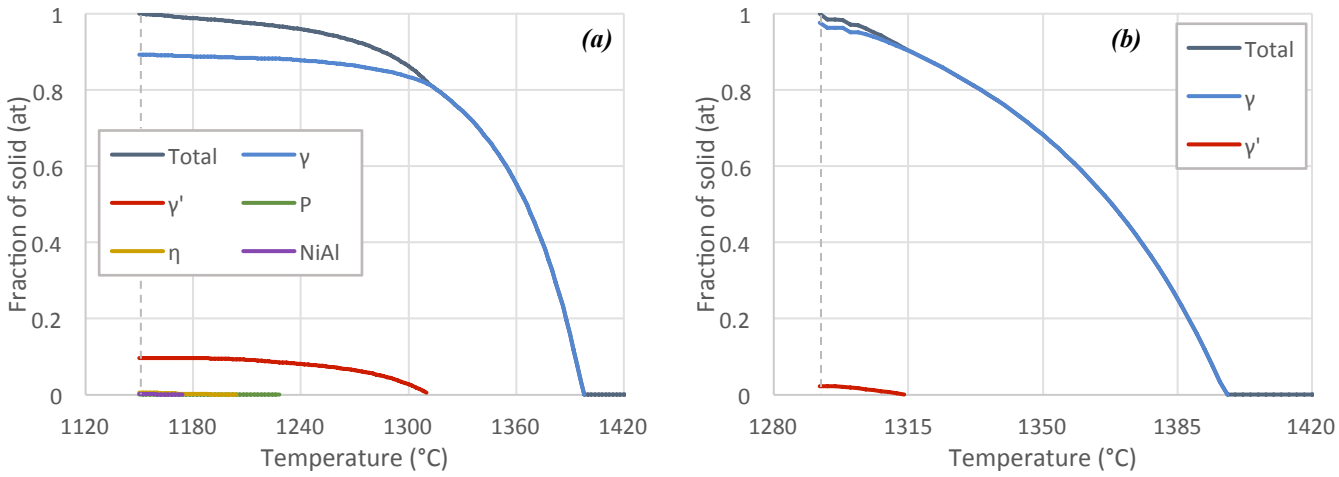

Figure 3: *Contributions of primary and secondary phases to the total fractions of solid obtained during solidification using Scheil-Gulliver (a) and back diffusion (b) models for the Ni-based superalloy René N6.*

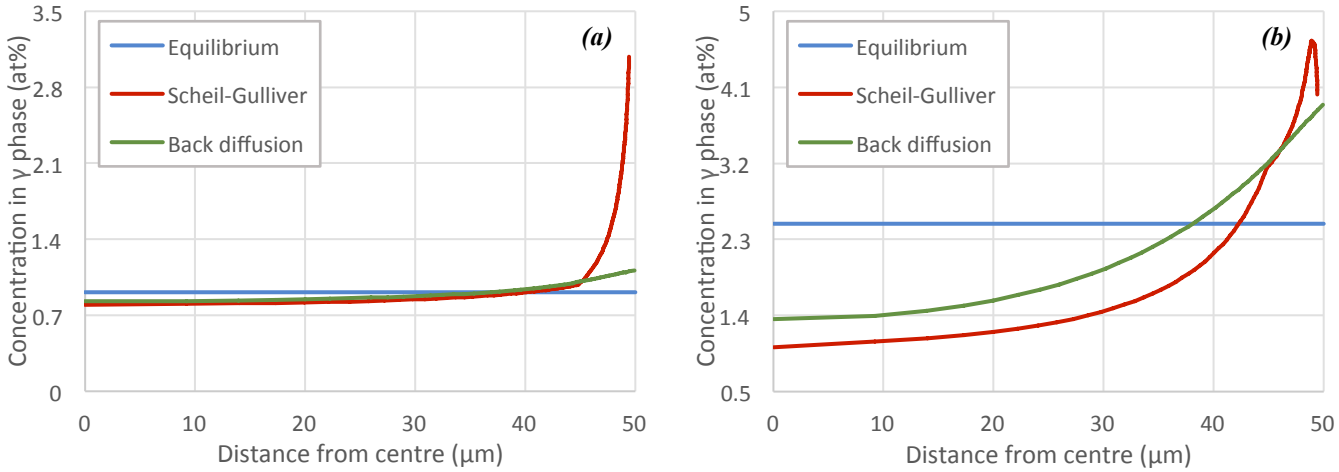

Figure 4: *Concentration profiles obtained at the end of solidification using equilibrium, Scheil-Gulliver, and back diffusion models for components Mo (a) and Ta (b) of the Ni-based superalloy René N6.*

corresponding value of 100 μm was used for the secondary dendrite arm spacing. The results are in striking contrast to those of Fig. 1, as the back diffusion predictions for these alloys fall in between the equilibrium and Scheil-Gulliver ones.

The case of the Ni-based superalloy René N6 is particularly instructive to highlight the importance of back diffusion. Figure 3 shows the breakdown of the total fractions of solid into contributions from primary and secondary phases, calculated for the whole freezing range of this alloy with Scheil-Gulliver and back diffusion models. It is seen that including back diffusion leads to a considerable reduction in the fraction of eutectic γ' that is ultimately obtained, with profound implications on the choice of heat treatment schedules. Additionally, since the solidus is located well above the Scheil-Gulliver prediction, three other secondary phases (P, η, and NiAl) are not formed at all. Not surprisingly, back diffusion also leads to more homogeneous solute concentration profiles, as illustrated in Fig. 4 for components Mo and Ta. This effect is more noticeable for faster diffusing elements, such as Mo in γ phase.

References

1. M. C. Flemings, *Solidification Processing*, McGraw-Hill: New York (1974)
2. N. Saunders, "Modelling of solidification in Al-alloys", in *Light Metals 1997*, edited by R. Huglen (TMS, 1997), p. 911

3. N. Saunders, “Applicability of the equilibrium and ‘Scheil model’ to solidification in multi-component alloys”, in *Solidification Processing 1997*, edited by J. Beech and H. Jones (University of Sheffield, 1997), p. 362

4. D. Larouche, “Computation of solidification paths in multiphase alloys with back-diffusion”, *CALPHAD: Computer Coupling of Phase Diagrams and Thermochemistry* **31**, 490 (2007)

5. N. Saunders, Z. Guo, X. Li, A. P. Miodownik, and J.-Ph. Schillé, “Using JMatPro to model materials properties and behavior”, *JOM* **55**, 60 (2003)

6. J. Guo and M. T. Samonds, “Alloy thermal physical property prediction coupled computational thermodynamics with back diffusion consideration”, *Journal of Phase Equilibria and Diffusion* **28**, 58 (2007)

7. P. G. Shewmon, *Diffusion in Solids*, McGraw-Hill: New York (1963)

8. J. Crank, *The Mathematics of Diffusion*, Clarendon Press: Oxford (1975)

9. Z. Guo, N. Saunders, P. Miodownik, and J.-Ph. Schillé, “Prediction of room temperature mechanical properties in aluminium castings”, in *Aluminium Alloys: Their Physical and Mechanical Properties*, edited by J. Hirsch, B. Skrotski, and G. Gottstein (Wiley, 2008), p. 1204

10. H. S. Whitesell, L. Li, and R. A. Overfelt, “Influence of solidification variables on the dendrite arm spacings of Ni-based superalloys”, *Metallurgical and Materials Transactions B* **31**, 546 (2000)